

Application of ion imaging to the atom-molecule exchange reaction: $\text{H} + \text{HI} \rightarrow \text{H}_2 + \text{I}$

Mark A. Buntine,^{a)} David P. Baldwin, Richard N. Zare,^{a)} and David W. Chandler
Combustion Research Facility, Sandia National Laboratories, Livermore, California 94551

(Received 27 November 1990; accepted 15 January 1991)

One of the ultimate goals in the field of reaction dynamics¹ is to be able to measure the angular distribution of products in a quantum-state-specific manner. As a step in this direction, we report the first application of ion imaging^{2,3} to a bimolecular reaction. We study the $\text{H} + \text{HI} \rightarrow \text{H}_2 + \text{I}$ reaction in a neat supersonic molecular beam of HI. The supersonic expansion provides a reaction precursor possessing a very narrow thermal velocity distribution. By avoiding a thermally equilibrated HI source (e.g., an effusive beam, or bulb), the center-of-mass collision energy spread has been substantially reduced. Fast H atoms are formed by laser photolysis of HI,⁴ and the H_2 ($v=1, J=11,13$) products are ionized by (2+1) resonance-enhanced multiphoton ionization (REMPI)⁵ before being imaged onto a position-sensitive detector. In this way we have measured the laboratory-frame velocity distribution of the state-selected reaction products. Early dynamical studies of the $\text{H} + \text{HI}$ abstraction reaction attempted to measure the angular distribution of the molecular product but failed because of background problems.^{6,7} More recently, internal state distributions of the molecular product have been determined, but without angular information.⁸⁻¹⁰

The experimental apparatus is conceptually the same as previously reported.^{11,12} Figure 1 shows a schematic diagram of the apparatus. A supersonic expansion of neat HI (Matheson, stated purity 98.0%, used without further purification) is introduced into a vacuum chamber through a pulsed valve (Series 9, General Valve Corp.) with a 0.8 mm diameter orifice. The backing pressure behind the nozzle is maintained at 950 Torr, while the base pressure in the chamber is typically 5×10^{-5} Torr. The molecular beam is collimated by a 0.7-mm diameter skimmer before entering the reaction and detection region in which the operating pressure is 8×10^{-8} Torr.

Approximately 5 cm downstream from the nozzle orifice, the molecular beam is intersected by a focused tunable laser beam (217–219 nm) whose linear polarization axis lies either parallel or perpendicular to the molecular beam axis. Photolysis of HI and detection of H_2 occur during the same laser pulse, which is approximately 5 ns in duration.¹³ The photodissociation process generates translationally hot H atoms with center-of-mass collision energies of approximately 2.6 and 1.7 eV. The two H-atom energies corresponds to competing photodissociation channels leading to the production of $\text{I}(^2P_{3/2})$ and $\text{I}^*(^2P_{1/2})$, respectively. The collision energy depends upon the photolysis wavelength, varying as different rovibrational levels of H_2 are detected.¹³ As the classical barrier to reaction is

only 0.04 eV,¹⁴ both H-atom channels can contribute to reaction.

Nascent H_2 product from the title reaction is detected via (2+1) REMPI. In this process, the H_2 molecules resonantly absorb two photons causing a transition from the $X^1\Sigma_g^+$ ($v''=1, J''=11,13$) ground state to the $E, F^1\Sigma_g^+$ ($v'_E=0, J'=J''$) excited electronic state. Here $v'_E=0$ denotes the lowest vibrational level in the E well of the E, F state.¹⁵ Subsequent absorption of an additional photon of the same wavelength leads to ionization. The H_2^+ ions are accelerated into a 14-cm time-of-flight tube and impinge upon a position-sensitive detector (Galileo). Ion images are obtained in an analogous manner to that discussed in detail in Ref. 11 with one important modification. The Doppler profile of H_2 produced in the title reaction is larger than the bandwidth of the ionization laser, necessitating the scanning of the frequency of this laser while an image is being collected.³ We assume that the photodissociation dynamics do not change significantly as the laser frequency is scanned over the Doppler profile.

Previous studies⁸⁻¹⁰ have shown that the vibrational distribution of the product H_2 is strongly inverted and peaks in $v=1$, and the $v=1$ rotational distribution peaks at $J=11$. This situation makes the $\text{H} + \text{HI}$ reaction particularly amenable to study because a relatively strong reactive product signal can be collected free of thermal H_2 background. We have recorded images showing the laboratory-frame velocity distribution of H_2 formed in $X^1\Sigma_g^+$ ($v=1, J=11,13$) quantum states. Figure 2 shows an image collected from product formed in the $J=11$ state. All images recorded, both in the $J=11$ and $J=13$ product states and with the laser polarized either parallel

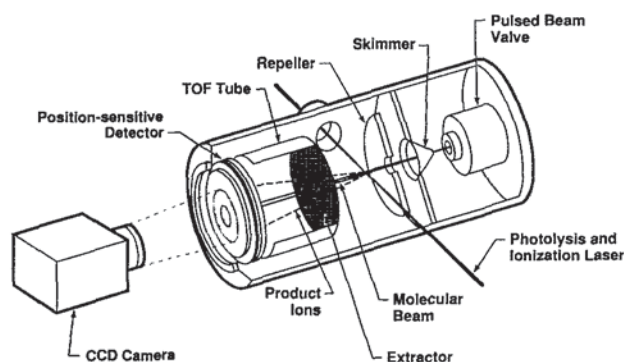


FIG. 1. Schematic diagram of the experimental apparatus.



FIG. 2. Ion image of H_2 ($v=1, J=11$) formed in the reaction $H + HI \rightarrow H_2 + I$ initiated in a beam of neat HI. Fast H atoms are formed by laser photolysis of HI, and the H_2 products are ionized by $(2+1)$ REMPI before being projected onto a position-sensitive detector. The ion density is represented by a continuous grey scale (white being highest intensity).

or perpendicular to the molecular beam axis, have nearly the same appearance as the image presented here. The fact that nearly identical images are obtained irrespective of the polarization of the laser indicates that the experimentally observed H_2 angular distribution is almost isotropic in space. This observation can be explained in part by considering the HI photodissociation dynamics. Photodissociation of HI at 217 nm generates translationally hot H atoms from competing parallel- and perpendicular-type dissociation pathways.^{4,16,17} H atoms formed along with $I^*(^2P_{1/2})$ (parallel dissociation) possess a $\cos^2 \theta$ spatial distribution and a recoil velocity of 1.72 eV, and H atoms formed along with $I(^2P_{3/2})$ (perpendicular dissociation) possess a $\sin^2 \theta$ spatial distribution (θ is the angle with respect to the laser polarization axis) and a recoil velocity of 2.66 eV. Levy and Shapiro¹⁶ calculate the I/I^* branching ratio to be approximately 5:3 in the wavelength region employed for this study. Van Veen *et al.*¹⁷ estimate the same ratio to be 4:3, indicating an almost equal propensity for both dissociation pathways.

There are two distinct regions clearly evident in Fig. 2: a bright central spot indicative of H_2 formed with relatively little translational energy, and a large outer ring corresponding to H_2 molecules that are moving quite rapidly. Figure 3 shows an intensity profile of Fig. 2, taken as a thin vertical slice down the center of the image. This profile clearly differentiates between the velocity distribution of

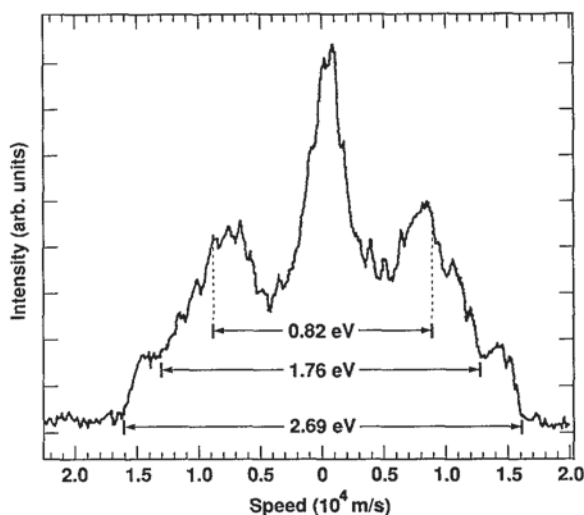


FIG. 3. Intensity profile of Fig. 2, taken as a thin vertical slice down the center of the image. Hydrogen molecules with a speed in excess of 0.5×10^4 m/s are products of the $H + HI \rightarrow H_2 + I$ reaction. Markers indicate the speeds of H_2 ($v=1, J=11$) products arising from reaction of HI with 2.63-eV and 1.70-eV H atoms (see text).

the "slow" H_2 and that of the faster moving product. As will be discussed later, we attribute the production of the slow H_2 to cluster chemistry in the molecular beam, while the faster moving hydrogen is produced from the title reaction.

A number of experiments have been performed under varying laboratory conditions giving us confidence that our images faithfully reproduce the velocity distribution of reaction products. To assure ourselves that the size of an image (and therefore the measured speed of the H_2) is not distorted by a "Coulomb explosion" following the ionization process, we recorded images at several different laser powers from approximately 0.2 to 1.5 mJ/pulse. If too many positive ions were produced in a given laser pulse, they would mutually repel, giving each ion an added velocity component. In the range of laser fluences employed, the size of the images did not change with laser power, assuring us that the data are not subject to errors associated with Coulomb distortion.

Images are typically recorded under experimental conditions that discriminate against the production of the low kinetic energy hydrogen molecules (observed as the bright central spot in Fig. 2). Primarily, this is achieved by having the laser intersect the leading edge of the pulsed molecular beam. Further suppression is achieved by warming the nozzle body to about 50 °C. Under these conditions the intensity of the central feature has been reduced by an order of magnitude from its maximum. Meanwhile, the intensity of the high-speed component of the signal is reduced by only about a factor of 2.5. Total suppression of the central feature could not be achieved. If we allow the intensity of the central spot to become too large, it overwhelms the outer ring, causing a distortion in the image size.

To assure self-consistency in our data, images are also recorded from the ($\nu = 1, J = 13$) state. Any artifacts in the REMPI detection scheme from the ($\nu = 1, J = 11$) state, for example an accidental degeneracy with a high rotational level in the $\nu = 0$ manifold, would be avoided by ionizing H_2 product in a different rovibrational level. We find that the H_2 ($\nu = 1, J = 13$) image is very similar to that of the H_2 ($\nu = 1, J = 11$) image; moreover, the smaller image size proves consistent with the reduction in energy available for product translation.

The $\text{H} + \text{HI}$ reaction is exothermic by 1.42 eV.¹⁴ Formation of H_2 ($\nu = 1, J = 11$) from the title reaction with little translational energy is not possible. Ionization of contaminant hydrogen in the molecular beam could account for a narrow distribution of H_2 with little kinetic energy. However, the thermal population of H_2 in this excited rovibrational level is too small to explain the central spot in the images. We have found that the exact size of this central area is clearly dependent on the molecular beam conditions and is seen at beam densities where the abstraction reaction signal (outer channel) is not observed. The origin of this slow H_2 remains to be established. We speculate on several mechanisms that could lead to production of such translationally cold and vibrationally and rotationally excited H_2 . First, the molecular product may be produced in conjunc-

tion with electronically excited I_2 from the dissociation of HI dimers formed in the molecular beam. Cho, Polanyi, and Stanners¹⁸ have also observed H_2 from photoreaction of adsorbed HX which they attribute to a similar mechanism. It is interesting to note that Sapers, Vaida, and Naaman¹⁹ observe the formation of I_2 in photodissociation studies of neat methyl iodide in a pulsed molecular beam. Moreover, rovibrationally excited H_2 may be formed from HI dimers with a symmetric IHHI transition state, in a configuration similar to the stable IHI complex.²⁰ In addition, the H_2 may be produced within a larger HI cluster before diffusing to, and evaporating from, the cluster surface. A further possible mechanism involves H_2 production from reactions of the type $\text{H} + (\text{HI})_n \rightarrow \text{H}_2 + \text{I} + (\text{HI})_{n-1}$, where the reactant H atoms are generated from HI photolysis.

Early kinetics studies of the $\text{H}(\text{thermal}) + \text{HI} \rightarrow \text{H}_2 + \text{I}^*$ reaction were carried out by Cadman and Polanyi.²¹ These workers monitored $\text{I}^* \rightarrow \text{I}$ infrared emission in a flow system and interpreted their results as meaning that essentially no $\text{I}^*(^2P_{1/2})$ is produced in the abstraction reaction, even though its formation is energetically possible. To date, no further studies into the product I^*/I branching ratio have been performed. If atomic iodine is formed exclusively in its ground electronic state by the $\text{H} + \text{HI}$ reaction, at the collision energies employed here (2.63 and 1.70 eV), we expect H_2 product formed in ($\nu = 1, J = 11$) to possess 2.69 and 1.76 eV of translational energy (the I atom recoil velocity is negligible compared to that of the H_2 product). If I atoms are formed in the $^2P_{1/2}$ excited electronic state by the $\text{H} + \text{HI}$ reaction, the associated H_2 product would possess 1.76 and 0.82 eV of translational energy.

As long as the arrival time at the detector is known, the speed of the fastest H_2 molecules in a given rovibrational state can be determined from the width of an image intensity profile. The greatest error in determining this speed arises from uncertainty in measuring the image size. Errors associated with measuring ion arrival times are insignificant. From Fig. 3 we calculate that the fastest H_2 ($\nu = 1, J = 11$) molecules possess 2.72 ± 0.05 eV of translation energy. This is in agreement with the 2.69 eV expected from reaction between HI and 2.63-eV H atoms, concomitant with ground state I atom production. Closer inspection of Fig. 3 shows that the wings of the intensity profile contain well defined shoulders, with a spacing between them corresponding to H_2 ($\nu = 1, J = 11$) molecules possessing 1.76 ± 0.04 eV of translational energy. Clearly this is in excellent agreement with the expected speed from reaction between HI and 1.70-eV H atoms, with I atoms formed in the ground electronic state. However, within the experimental uncertainty of data presented in Fig. 3, we cannot unambiguously distinguish between this pathway and reaction between HI and 2.63-eV H atoms resulting in H_2 formation in conjunction with $^2P_{1/2}$. In Fig. 3 we have marked the spacing expected for the onset of H_2 ($\nu = 1, J = 11$) formed in conjunction with I^* , resulting from reaction between HI and the 1.70-eV H atoms (those produced along with I^* from HI photolysis). Preliminary

analysis of this data (which includes a reconstruction of the 3-D product velocity distribution) seems to indicate that the "I* + I*" reaction channel is indeed active at these collision energies. Further analysis should provide information relating to the product I*/I branching ratio.

We have demonstrated an ability to acquire undistorted ion images of molecular products from a bimolecular reaction in a single supersonic molecular beam. The supersonic expansion has enabled us to reduce substantially the center-of-mass collision energy spread compared to studies performed using room-temperature reagent sources. The ion images record the laboratory-frame velocity distribution of state-selected reaction products. Moreover, we have been able to distinguish between products formed from competing reaction channels. All of this makes us confident that it should be possible, with improvements in the duty cycle, to carry out ion imaging experiments with separated molecular beams for the reactants, thus permitting the determination of doubly differential reaction cross sections, that is, determination of both the internal state and scattering velocity distributions.

We would like to thank Mark Jaska for his expert technical support throughout the course of this project. This work is supported by the U.S. Department of Energy, Office of Basic Energy Sciences, Division of Chemical Sciences. M.A.B. and R.N.Z. would like to acknowledge support from the National Science Foundation (under Contract Number NSF CHE 90-07939).

^{a1}Department of Chemistry, Stanford University, Stanford, California 94306.

¹R. D. Levine and R. B. Bernstein, *Molecular Reaction Dynamics and Chemical Reactivity* (Oxford University Press, City, 1987).

²D. W. Chandler and P. L. Houston, *J. Chem. Phys.* **87**, 1445 (1987).

³J. W. Thoman, Jr., D. W. Chandler, D. H. Parker, and M. H. M. Janssen, *Laser Chem.* **9**, 27 (1988).

⁴R. D. Clear, S. J. Riley, and K. R. Wilson, *J. Chem. Phys.* **63**, 1340 (1975); R. Schmiedl, H. Dugan, W. Meier, and K. H. Welge, *Z. Phys. A*, **304**, 137 (1982).

⁵W. M. Huo, K.-D. Rinnen, and R. N. Zare (submitted to *J. Chem. Phys.*); K.-D. Rinnen, M. A. Buntine, D. A. V. Kliner, R. N. Zare, and W. M. Huo (submitted to *J. Chem. Phys.*).

⁶J. D. McDonald and D. R. Herschbach, *J. Chem. Phys.* **62**, 4740 (1975).

⁷W. Bauer, L. Y. Rusin, and J. P. Toennies, *J. Chem. Phys.* **68**, 4490 (1978); W. H. Beck, R. Götting, J. P. Toennies, and K. Winkelmann, *ibid.* **72**, 2896 (1980).

⁸P. M. Aker, G. J. Germann, and J. J. Valentini, *J. Chem. Phys.* **90**, 4795 (1989); P. M. Aker, G. J. Germann, K. D. Tabor, and J. J. Valentini, *ibid.* **90**, 4809 (1989).

⁹D. A. V. Kliner, K.-D. Rinnen, and R. N. Zare, *J. Chem. Phys.* **90**, 4625 (1989); K.-D. Rinnen, D. A. V. Kliner, M. A. Buntine, and R. N. Zare, *Chem. Phys. Lett.* **169**, 365 (1990).

¹⁰D. A. V. Kliner, K.-D. Rinnen, M. A. Buntine, D. E. Adelman, and R. N. Zare (submitted to *J. Chem. Phys.*).

¹¹D. P. Baldwin, M. A. Buntine, and D. W. Chandler, *J. Chem. Phys.* **93**, 6578 (1990).

¹²D. W. Chandler, J. W. Thoman, Jr., M. H. M. Janssen, and D. H. Parker, *Chem. Phys. Lett.* **156**, 151 (1989); D. W. Chandler, M. H. M. Janssen, S. Stolte, R. N. Strickland, J. W. Thoman, Jr., and D. H. Parker, *J. Phys. Chem.* **94**, 4839 (1990).

¹³K.-D. Rinnen, D. A. V. Kliner, R. S. Blake, and R. N. Zare, *Chem. Phys. Lett.* **153**, 371 (1988).

¹⁴M. Baer and I. Last, in *Potential Energy Surfaces and Dynamics Calculations*, edited by D. G. Truhlar (Plenum, New York, 1981).

¹⁵T. E. Sharp, *At. Data* **2**, 119 (1971).

¹⁶I. Levy and M. Shapiro, *J. Chem. Phys.* **89**, 2900 (1988).

¹⁷G. N. A. Van Veen, K. A. Mohamed, T. Baller, and A. E. De Vries, *Chem. Phys.* **80**, 113 (1983).

¹⁸C.-C. Cho, J. C. Polanyi, and C. D. Stanners, *J. Chem. Phys.* **90**, 598 (1989).

¹⁹S. P. Sapers, V. Vaida, and R. Naaman, *J. Chem. Phys.* **88**, 3638 (1988).

²⁰C. Kubach, *Chem. Phys. Lett.* **164**, 475 (1989), and references therein.

²¹P. Cadman and J. C. Polanyi, *J. Phys. Chem.* **72**, 3715 (1968).